

# Pair approximation models for disease spread

J. Benoit<sup>a</sup>, A. Nunes, and M. Telo da Gama

Centro de Física Teórica e Computacional e Departamento de Física, Faculdade de Ciências da Universidade de Lisboa, Avenida Professor Gama Pinto 2, 1649-003 Lisboa, Portugal

Received 12 October 2005 / Received in final form 24 November 2005

Published online 12 April 2006 – © EDP Sciences, Società Italiana di Fisica, Springer-Verlag 2006

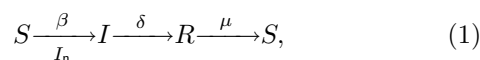
**Abstract.** We consider a Susceptible-Infective-Recovered (SIR) model, where the mechanism for the renewal of susceptibles is demographic, on a ring with next nearest neighbour interactions, and a family of correlated pair approximations (CPA), parametrized by a measure of the relative contributions of loops and open triplets of the sites involved in the infection process. We have found that the phase diagram of the CPA, at fixed coordination number, changes qualitatively as the relative weight of the loops increases, from the phase diagram of the uncorrelated pair approximation to phase diagrams typical of one-dimensional systems. In addition, we have performed computer simulations of the same model and shown that while the CPA with a constant correlation parameter cannot describe the global behaviour of the model, a reasonable description of the endemic equilibria as well as of the phase diagram may be obtained by allowing the parameter to depend on the demographic rate.

**PACS.** 02.50.-r Probability theory, stochastic processes, and statistics – 87.23.Ge Dynamics of social systems – 05.70.Ln Nonequilibrium and irreversible thermodynamics

## 1 Introduction

Stochastic Susceptible-Infective-Recovered (SIR) epidemic models on lattices and networks can be mapped on to percolation problems and are well understood [1–3]. To describe disease spread and persistence in a community, the model must be extended to include a mechanism for renewal of susceptibles, either births or immunity waning.

Models with immunity waning, Susceptible-Infective-Recovered-Susceptible (SIRS), are based on the following transitions:



meaning that any susceptible individual  $S$  can be infected by an infected neighbour  $I_n$  at the infection rate  $\beta$ , any infected individual  $I$  becomes recovered  $R$  at the recovery rate  $\delta$ , and any recovered individual  $R$  becomes susceptible  $S$  at the immunity loss rate  $\mu$ . Following customary habits, we shall choose time units for which  $\delta = 1$ .

The SIRS model interpolates between two well known models, the contact process (also known as Susceptible-Infective-Susceptible or SIS) and the SIR model, in the limits  $\mu \rightarrow \infty$  and  $\mu \rightarrow 0$ , respectively, and much is known about its behaviour on regular lattices, both from the point of view of rigorous results [4–6] and of assessing

the performance of mean field and pair approximations against stochastic simulations [7].

In particular, it is known [6] that on hypercubic lattices of arbitrary dimension the phase diagram of (1) has two critical values,  $\beta_c(\infty) < \beta_c(0)$ , which are the critical rates of the two limit problems that is the contact process and SIR, respectively. For  $\beta < \beta_c(\infty)$  there is disease extinction for every  $\mu$ , while for  $\beta_c(0) < \beta$  there is disease persistence for every  $\mu$ . For  $\beta_c(\infty) < \beta < \beta_c(0)$  disease persistence occurs only for  $\mu$  above a certain threshold. The region of disease persistence for every  $\mu$  is ‘missing’ in dimension  $d = 1$ , because in this case  $\beta_c(0)$  is infinite.

In [7] the uncorrelated pair approximation (UPA, see Sect. 2) was applied to the SIRS model (1) on linear and square lattices, and the phase diagrams computed from the corresponding equations of evolution were compared with the mean field phase diagram and with the results of simulations. It was shown that, by contrast with the mean field approximation, the UPA phase diagram agrees qualitatively with the simulations and the exact results both in  $d = 1$  and in  $d = 2$ .

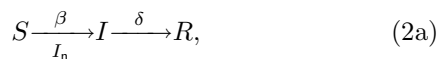
Since the UPA does not take into account the lattice dimensionality explicitly, it predicts identical phase diagrams on lattices with the same coordination number  $k$ , namely on linear ( $d = 1$ ) and square ( $d = 2$ ) lattices, when next nearest neighbours ( $k = 4$ ) are considered. However, in one dimension the critical infection rate  $\beta_c(0) = \infty$ ,

<sup>a</sup> e-mail: benoit@cii.fc.ul.pt

and the critical line has an asymptote at  $\mu = 0$ , while in two dimensions the critical line crosses the  $\mu = 0$  axis at a finite value of  $\beta_c$ , which is the result of the UPA for  $k = 4$ .

The question is then whether generalized pair approximations can account for the dependence on dimensionality and, in particular, whether they can describe phase diagrams with different qualitative behaviours at fixed coordination numbers.

We have addressed this question, and more generally the problem of constructing suitable pair approximations (Sect. 2), in the context of a modification of model (1), where the mechanism of renewal of susceptibles is demography, rather than immunity waning. This is the natural scenario in the epidemiology of diseases that confer permanent immunity, such as childhood infectious diseases [8, 9]. For this model infection obeys the same rules as in (1), immunity is permanent and all individuals, whatever their state, are submitted to birth and death events at a rate  $\mu$ . The stochastic process, which describes the dynamics of this system, is governed by the transitions



In the limit  $\mu = 0$ , both models (1) and (2) coincide with SIR model. In the opposite limit the dynamics of the two models are drastically different. While, in the limit  $\mu = \infty$ , SIRS coincides with the contact model [7], in the same limit the dynamics of (2) is trivial: it is driven by demography, that keeps the entire population susceptible for any  $\beta_c$ , and thus  $\beta_c(\infty) = \infty$ . We are interested in the regime, where  $\mu$  is smaller than the recovery rate, which is meaningful for the study of acute disease spread. Although in this regime the dynamics is dominated by the infection and recovery processes which are identical in both models, the behaviour of (2) appears to be different, in a subtle way, from that of (1) (Sect. 2).

We have considered the demographic SIR model (2) on a linear lattice with periodic boundary conditions (ring) and next nearest neighbour interactions,  $k = 4$ . We constructed a family of correlated pair approximations (CPA), parametrized by  $\theta$ , a measure of the relative contributions of loops and open triplets of connected sites involved in the disease spread (Sect. 3). For  $\theta = 0$  the approximation reduces to the standard UPA (Sect. 2). The phase diagrams of the CPA show that as  $\theta$  increases from 0 to  $\theta^*$  (see Sect. 3) the CPA interpolates between the  $k = 4$  UPA critical behaviour and the typical one-dimensional phase behaviour, with  $\beta_c(0) = \infty$ . Finally, we have simulated the demographic SIR model (2) on a ring, with  $k = 4$ . The results of the simulations indicate that while the CPA with a constant value of  $\theta$  cannot describe the global phase diagram of (2), a reasonable description of endemic equilibria as well as of the phase diagram is obtained when  $\theta$  is allowed to depend on the demographic rate  $\mu$  (Sect. 3). This illustrates that in addition to describe the dimensional crossover for lattices

with coordination number  $k = 4$ , the CPA can be made semi-quantitative providing an alternative to the stochastic simulations of individual based models. We conclude in Section 4 with a brief discussion of the results.

## 2 Mean field and uncorrelated pair approximations

In this section we consider the time evolution of the demographic SIR model on regular lattices and review the mean-field and (standard) uncorrelated pair approximations, setting the notation and the stage for the development of the more sophisticated correlated pair approximations.

In the demographic SIR model on networks, sites represent individuals and bonds social links. The dynamics is governed by the stochastic process (2). Denoting by  $P_t(A)$  the probability for an individual to be in state  $A$  (at time  $t$ ),  $P_t(AB)$  the probability for a lattice bond to connect an individual in state  $A$  to an individual in state  $B$ , the time evolution of the singleton probabilities  $P_t(A)$  can be described by the set of first order differential equations [8, 9]:

$$\frac{dP_t(S)}{dt} = +\mu [P_t(I) + P_t(R)] - \beta \sum_n P_t(SI_n), \quad (3a)$$

$$\frac{dP_t(I)}{dt} = +\beta \sum_n P_t(SI_n) - (\mu + \delta) P_t(I), \quad (3b)$$

$$\frac{dP_t(R)}{dt} = +\delta P_t(I) - \mu P_t(R), \quad (3c)$$

where the summations run over the connected neighbours. Clearly the set of equations (3) is not closed since it involves pair probabilities without describing their time evolution. This follows from the stochastic process (2) where infection (2a) proceeds via  $SI$  contact pairs.

As a matter of fact, the time evolution of the  $q$ -tuple probabilities is described by a set of first order differential equations expressing their time derivatives as linear combinations of  $q$ -tuple and  $(q+1)$ -tuple probabilities, subject to a normalization condition. In order to proceed, the set of equations must be closed, that is the  $(q+1)$ -tuple probabilities must be written in terms of  $q$ -tuple probabilities. The ‘art’ is to use closures that capture key physical features of the system and are still manageable by symbolic or numerical-symbolic computation. The results of a particular closure, or approximation, may then be checked against rigorous results and/or stochastic simulations.

For most closures the  $(q+1)$ -tuple probabilities are rational functions of the  $q$ -tuple probabilities, appropriately normalized, and thus the constrained set of first order differential equations may be replaced by an unconstrained set where the time derivatives of independent  $q$ -tuple probabilities are expressed as rational functions of these  $q$ -tuple probabilities. Although the resulting sets of equations are easily integrable by classical numerical methods and admit polynomial systems as steady state

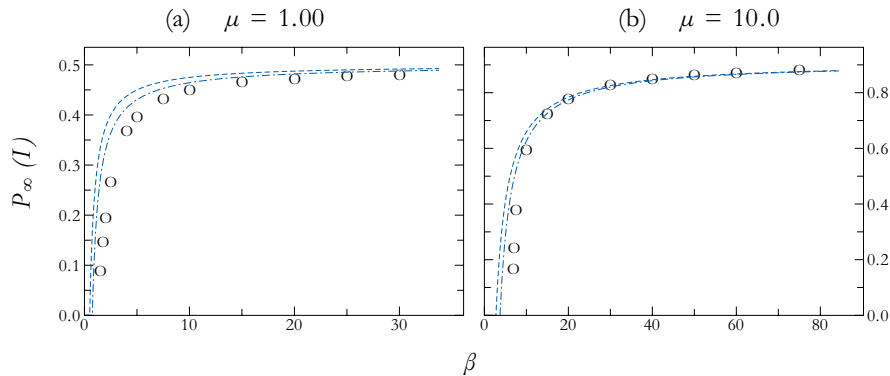


**Fig. 1.** Endemic infective probability versus infection rate at (a) high demographic rate, and at (b) huge demographic rate: the endemic infective probability is plotted from simulations (open circles), the MFA (long dashed lines), the UPA (dashed dotted lines) and the correlated model with best-fit closed form parameters (solid lines). The fitting procedure is based on perpendicular offsets and on the assumption that the closed form parameter  $\theta$  depends only on the demographic rate  $\mu$ . Closed form parameters  $\theta$  for (a) and (b) respectively: 0.50, 0.70.

equations, their analysis remains cumbersome even at low order  $q$ .

The simplest closure is the mean field approximation (MFA), where the pairs (2-tuples) are assumed to be formed by uncorrelated singletons (1-tuples):

$$\sum_n P_t(SI_n) \approx k P_t(S)P_t(I). \quad (4)$$

For the demographic SIR model the endemic equilibrium (steady state) is computed easily. The mean-field endemic infective probabilities are plotted in Figure 1 as a function of the infection rate, at two values of  $\mu$ . For any value of  $\mu$ , the MFA predicts two different steady states: at infection rates  $\beta$  smaller than the critical infection rate  $\beta_c$  there is disease extinction, while at infection rates  $\beta$  greater than the critical infection rate  $\beta_c$  there is disease persistence, i.e. infected (and recovered) individuals coexist with susceptibles. The two regimes are separated by the mean-field endemic threshold that is plotted in Figure 2 (dashed line).

We anticipate that the results of the MFA will be accurate when the demographic process of (2) dominates over the infectious one since in this regime pairs are continually broken and thus the behaviour of each individual is essentially independent on that of the other ones. The infection process governed by *Susceptible-Infected* contact pairs, dominates in the opposite regime ( $\mu \ll 1$ ), relevant in the epidemiological context. The appropriate mean field theory is then the uncorrelated pair approximation (UPA).

The UPA is for pairs what the MFA is for singletons. In the UPA triplets (3-tuples) are assumed to be formed by uncorrelated pairs:

$$\sum_n P_t(ASI_n) \approx (k-1) \frac{P_t(SA)P_t(SI)}{P_t(S)}. \quad (5)$$

The UPA is expected to outperform the MFA but, in general, its solution is not known in closed form. For the demographic SIR model the calculation of the phase diagram and the stability analysis is still tractable by symbolic computation. For lattices with coordination number

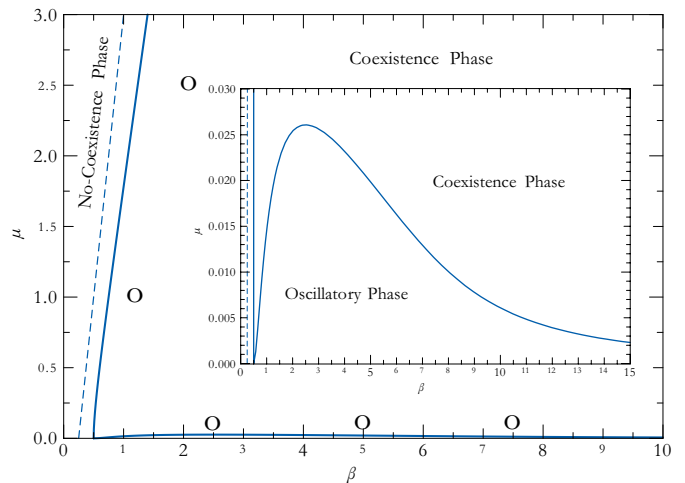


**Fig. 2.** Phase diagram for the UPA: the no-coexistence phase and the coexistence phase are separated by the critical curve from simulations (open circles), the MFA (long dashed line), and the UPA (thick solid line). Within the coexistence phase, at very low demographic rates  $\mu$ , the UPA predicts an oscillatory phase as shown in the inset.

$k = 4$ , the phase diagram is plotted in Figure 2. It is clear that the UPA is quantitatively superior to the MFA when compared with the results of simulations (open circles). Both the MF and the UP approximations of the  $k = 4$  demographic SIR model predict a finite critical infection rate at  $\mu = 0$ , while the simulations indicate that  $\beta_c$  will diverge as  $\mu$  tends to 0.

However, the SIRS and the demographic SIR models are different at low (but finite) demographic rates  $\mu$ . In the demographic SIR model the mechanism for the renewal of susceptibles is totally random by contrast to the mechanism of the SIRS model. In our model susceptibles are born anywhere on the lattice while in the SIRS model only previously infected sites loose immunity.

We note that the randomizing effect of the demographic SIR mechanism for the renewal of susceptibles is

reminiscent of the randomizing effect of shortcuts in small-world networks of the Watts and Strogatz type [10,11] where correlations are destroyed and an effective mixing of the population is achieved, with (drastic) consequences on the phase diagram.

Finally, it is worth noticing that the UPA also predicts the existence of an oscillatory phase within the survival or coexistence phase (i.e., to the right of  $\beta_c(0)$ ), for small values of  $\mu$  (Fig. 2). The same is true for the UPA of process (1) on the square lattice. This behaviour will be difficult to identify in stochastic simulations, since it may be blurred by large fluctuations and stochastic extinctions.

### 3 Correlated pair approximations

In order to construct more realistic pair approximations, we have investigated closure procedures inspired by the geometrical structure of the lattice.

Within this perspective and as far as social triplets are concerned, the ring of degree  $k = 4$  and the triangular lattice ( $k = 6$ ) are propitious networks since their nearest-neighbour triplets split into two distinct classes: ‘chain-like’ (open) and ‘loop-like’ (closed) triplets. A very naive idea is to take into account the two classes of triplets and to use the probability  $\theta$  and  $1 - \theta$  of finding respectively a ‘loop-like’ triplet and a ‘chain-like’ triplet as a parameter to be fitted to simulation results. Thus triplets are assumed to be formed either of uncorrelated (chained) pairs or of correlated (looped) pairs [12]:

$$\sum_n P_t(ASI_n) \approx \begin{cases} (k-1) \left[ (1-\theta) \frac{P_t(SA)P_t(SI)}{P_t(S)} + \theta \frac{P_t(AI)P_t(SA)P_t(SI)}{P_t(A)P_t(S)P_t(I)} \right] & \text{if } A \in \{S, R\}, \\ (k-1) P_t(SI) - \sum_n [P_t(SSIn) + P_t(RSIn)] & \text{if } A = I. \end{cases} \quad (6)$$

The demographic SIR version of the CPA (6) is amenable by cumbersome numerical-symbolic computation although some interesting results may be obtained by symbolic computation. The phase diagrams are shown in Figure 3. We find that, as  $\theta$  increases from 0 to  $\theta^* \approx 0.3807^1$ , keeping  $k = 4$  fixed, the CPA phase diagrams interpolate between the UPA behaviour and typical one-dimensional phase diagrams with  $\beta_c(0) = \infty$ . At  $\theta^*$  the critical infection rate  $\beta_c$  tends asymptotically to infinity as the demographic rate  $\mu$  vanishes. Inspection of Figure 3 also shows that the closed form parameter  $\theta$  cannot be constant if a quantitative description of the global phase diagram is required. If we allow  $\theta$  to depend on  $\mu$ , reasonable descriptions of the endemic equilibria (Fig. 1) and of the global phase diagram (Fig. 3) are obtained. For the

<sup>1</sup> the real solution of the cubic equation  $27\theta^3 - 18\theta^2 + 87\theta - 32 = 0$ .

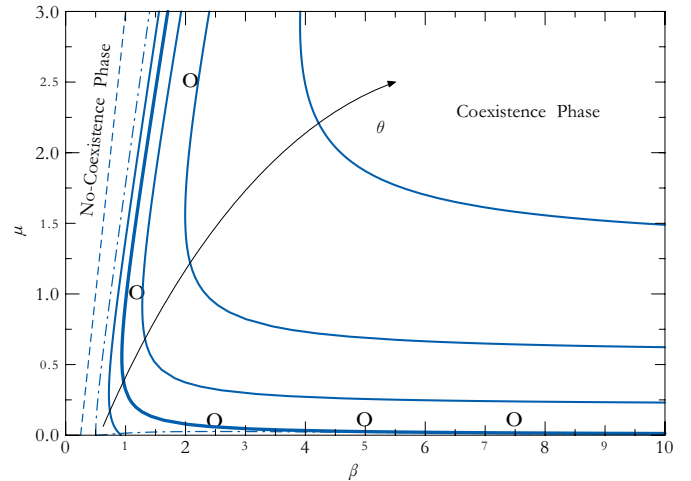


**Fig. 3.** Isoparametric phase diagrams for the correlated model: the no-coexistence and coexistence phases are separated by the critical curve from simulations (open circles), the MFA (long dashed line), the UPA (dashed dotted line) and the correlated model for different  $\theta$  (solid lines). For  $\theta^* \approx 0.3807$  (bold solid line) the critical infection rate  $\beta_c$  tends asymptotically to infinity when the demographic rate  $\mu$  vanishes. Closed form parameters  $\theta$  from left to right:  $\frac{1}{4}$ ,  $\theta^*$ ,  $\frac{1}{2}$ ,  $\frac{5}{8}$ ,  $\frac{3}{4}$ .

SIRS model (1) on the square lattice, a CPA obtained by fitting  $\theta$  to  $\beta_c(0)$  will improve the results of the UPA used in [7] to describe the behaviour of the system at low values of  $\mu$ .

### 4 Discussion

We have proposed a simple CPA that was shown to provide a reasonable approximation to the behaviour of stochastic models that are relevant in epidemiology — the agreement against simulation data being far better than MFA and UPA with a suitable choice of the parameters. The resulting equations of evolution may be used to approximate phase diagrams, as well as steady state and dynamical behaviours of the associated stochastic models. The CPA takes into account some of the effects of the local lattice structure and yields a clear alternative to heavy stochastic simulations.

One of the directions of future work includes the development of CPAs, along the lines of the present work, to account for the local (lattice like) structure of a class of complex networks, such as the Watts and Strogatz small-world networks, that have been shown to be relevant in epidemiological contexts [13].

Financial supports from the Foundation of the University of Lisbon, under contract BPD-CI/01/04, and from the Portuguese Foundation for Science and Technology (FCT), under contracts POCTI/ESP/44511/2002 and POCTI/ISFL/2/618, are gratefully acknowledged.

## References

1. P. Grassberger, *Math. Biosci.* **63**, 157 (1982)
2. C. Moore, M.E.J. Newman, *Phys. Rev. E* **61**, 5678 (2000), e-print [arXiv:cond-mat/9911492](#)
3. C. Moore, M.E.J. Newman, *Phys. Rev. E* **62**, 7059 (2000), e-print [arXiv:cond-mat/0001393](#)
4. R. Durrett, C. Neuhauser, *Ann. Appl. Probab.* **1**, 189 (1991)
5. E. Andjel, R. Schinazi, *J. Appl. Probability* **33**, 741 (1996)
6. J. van den Berg, G.R. Grimmett, R. B. Schinazi, *Ann. Appl. Probab.* **8**, 317 (1998)
7. J. Joo, J.L. Lebowitz, *Phys. Rev. E* **70**, 036114 (2004), e-print [arXiv:q-bio/0404035](#)
8. R.M. Anderson, R.M. May, *Infectious Diseases of Humans: Dynamics and Control* (Oxford University Press, Oxford, 1991)
9. J.D. Murray, *Mathematical Biology II: Spatial Models and Biomedical Applications*, Vol. 18 (Springer-Verlag, New-York, 2003), 3rd edn.
10. D.J. Watts, S.H. Strogatz, *Nature* **393**, 440 (1998)
11. M.B. Hastings, *Phys. Rev. Lett.* **91**, 098701 (2003), e-print [arXiv:cond-mat/0304530](#)
12. M. van Baalen, *Pair Approximations for Different Spatial Geometries* (Cambridge University Press, Cambridge, 2000), Vol. 1, Chapter 19, pp. 359–387
13. J. Verdasca, M. Telo da Gama, A. Nunes, N.R. Bernardino, J.M. Pacheco, M.C. Gomes, *J. Theoret. Biol.* **233**, 553 (2005), e-print [arXiv:q-bio/0408002](#)